Supporting Information
Molecular Transport Across Ionic Liquid–Aqueous Electrolyte Interface in a MoS_2 nanopore

Manish Shankla and Aleksei Aksimentiev*
Department of Physics, University of Illinois, 1110 W. Green St., Urbana, IL
*E-mail: aksiment@illinois.edu

Contents

Supporting Information Figures

Figure S1: Distribution of K^+ and Cl^- ions in phase separated system 2
Figure S2: Electrical charge profile of all molecular species in phase separated system . 3
Figure S3: Solvation energy of K^+ and Cl^- ions in IL-rich phase 4
Figure S4: Self-diffusion coefficients of water, PF_6 and BMIM in IL and AS phases . . . 5
Figure S5: Distribution of molecular species across IL/AS interface at equilibrium and at 200 mV 6
Figure S6: Evolution of the electrostatic potential in MoS_2 nanopore at 200 mV 7
Figure S7: Effect of MoS_2 force field on distribution of molecular species 8
Figure S8: Effect of MoS_2 force field on ionic current magnitude 9
Figure S9: Single nucleotide clustering in pure [Bmim][PF_6] and 1M KCl solution . . . 10
Figure S10: Single nucleotide diffusivity in pure [Bmim][PF_6] and 1M KCl solution . . . 11
Figure S11: Distribution of PF_6 and BMIM around single nucleotides in pure [Bmim][PF_6] 12
Figure S12: Average lifetime of PF_6 and BMIM binding to nucleotides 13
Figure S11: Distribution of PF_6 and BMIM around DNA homopolymers in pure [Bmim][PF_6] 14
Figure S14: Aggregation of hydrated nucleotides in IL 15

Captions to Supplementary Movies 16–23

Supplementary References 24

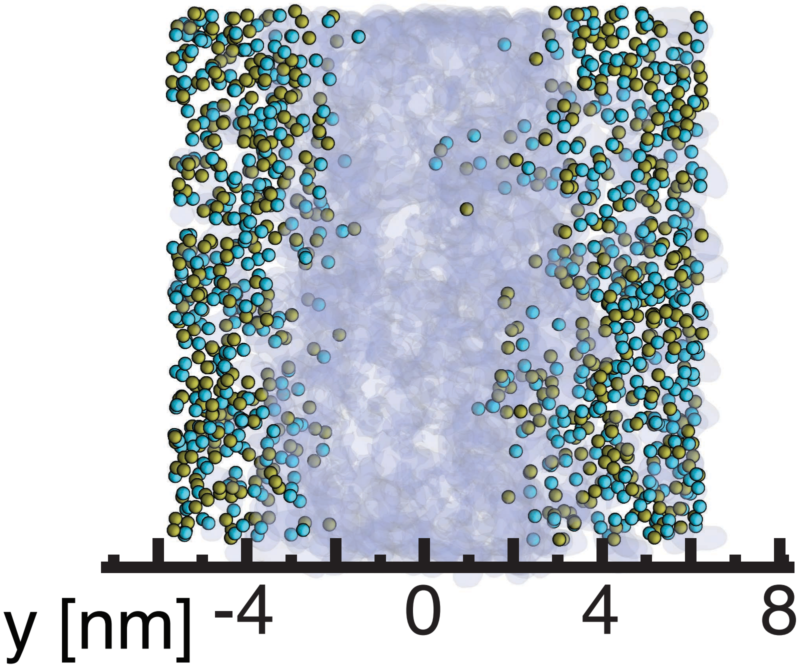

Figure S1. A 50/50 mixture of [Bmim][PF_6] and water at equilibrium. The BMIM and PF_6 molecules are shown using blue semi-transparent surfaces, K^+ and Cl^- ions as gold and cyan van der Waals (vdW) spheres, respectively, and water molecules are not shown for clarity.

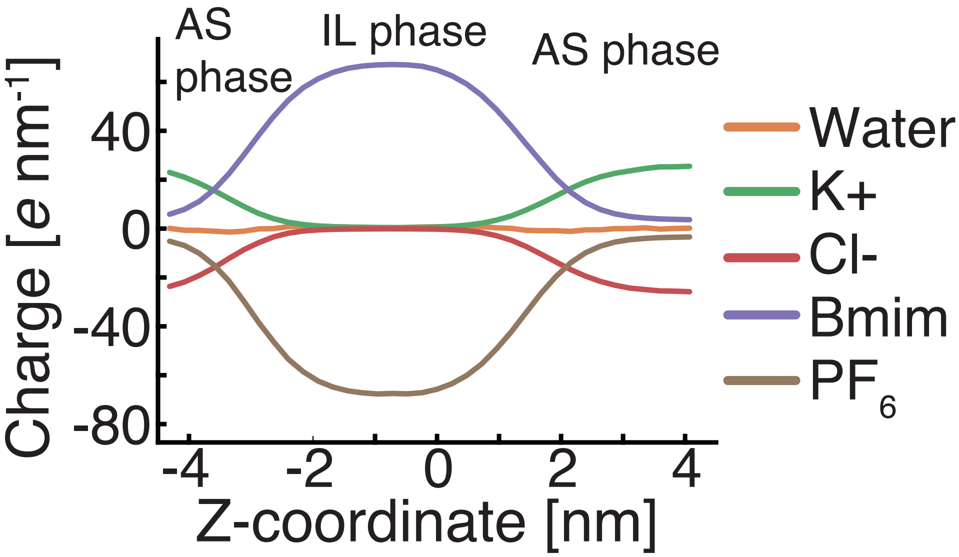

Figure S2. Equilibrium profile of the electrical charge density for each molecular species across the IL/AS interface as seen in the simulation of a 50/50 IL/AS mixture; the system is shown in Figure 1d. The profiles were averaged over the last 90 ns of the MD trajectory in 1.0 Å bins.

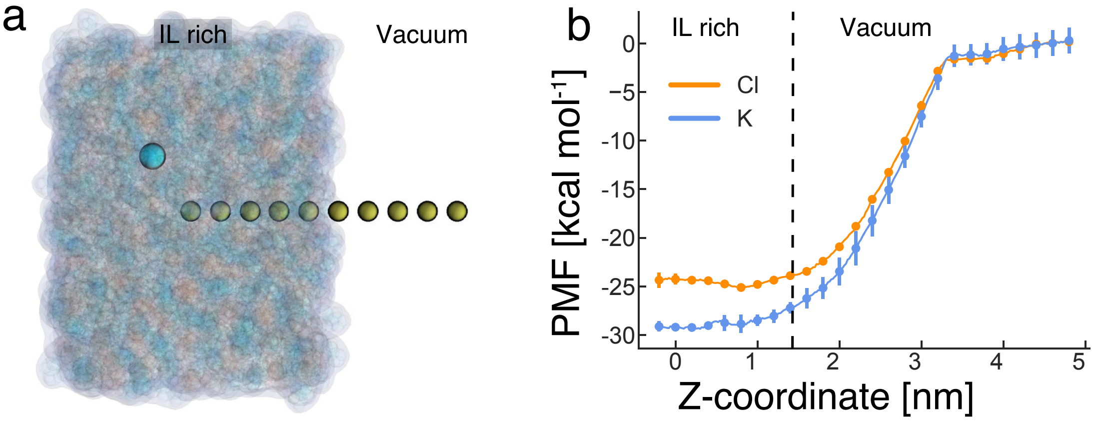

Figure S3. Solvation free energy of K^+ and Cl^- in IL-rich phase. The solvation free energy of $\Delta G_{\mathrm{Cl/K}} = G_{\mathrm{IL\ rich}} - G_{\mathrm{Vacuum}}$ was computed using the Adaptive Biasing Force (ABF) method [1] implemented in NAMD [2]. ABF calculates the free energy by estimating the average force applied by the system along the reaction coordinate while simultaneously applying opposite force until the evolution of the system along the reaction coordinate is governed by diffusion. Sampling along the reaction coordinate is enhanced by performing several simulations in parallel within multiple non-overlapping windows [3]. (a) Initial conditions illustrating the location of a K^+ or Cl^- ion (gold vdW sphere) in ten independent ABF simulation windows. Each simulation system contained a single K^+ or Cl^- ion initially placed in one of the ten locations and a single counterion (cyan vdW sphere) placed inside the IL-rich phase to ensure electrical neutrality of the system. The IL-rich phase was saturated with water molecules at ∼19% of bulk water density. In each ABF window, samples were collected in 0.2 Å bins and averaged over 2000 steps to determine the biasing force. Each ABF window was simulated for 12 ns. (b) Potential of mean force of a single Cl^- (orange line) and K^+ (blue line) ion across the IL rich/vacuum interface (dashed line).

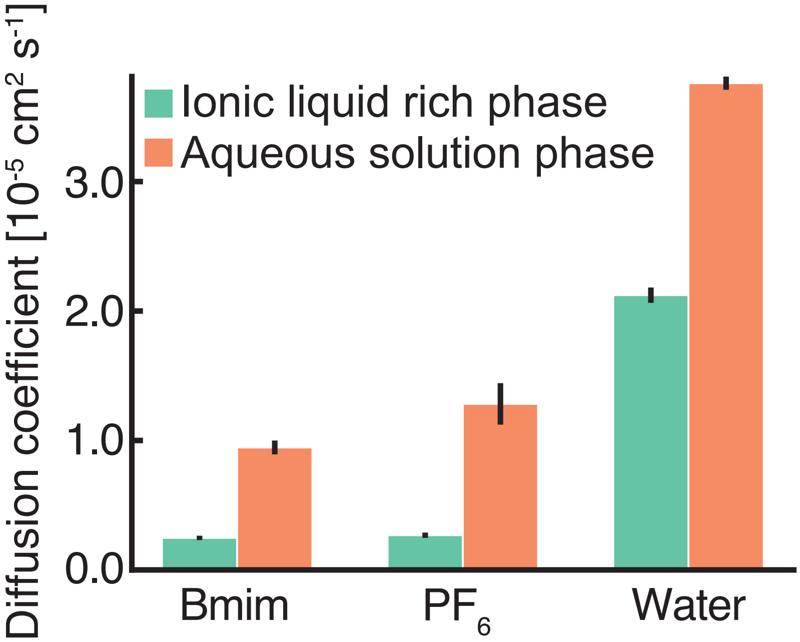

Figure S4. Self-diffusion coefficients of water, PF_6 and BMIM in the IL and AS phases. Mean squared displacement of each molecule was calculated from 1 ns segments of the trajectory. The diffusion coefficients for each segment were calculated by performing a linear least squares fit the MSD and taking 1/6 of the slope of the fitted lines. The diffusion coefficients from the independent segments were averaged to compute the mean diffusion coefficient. The error bars are the standard deviation of the mean diffusion coefficient.

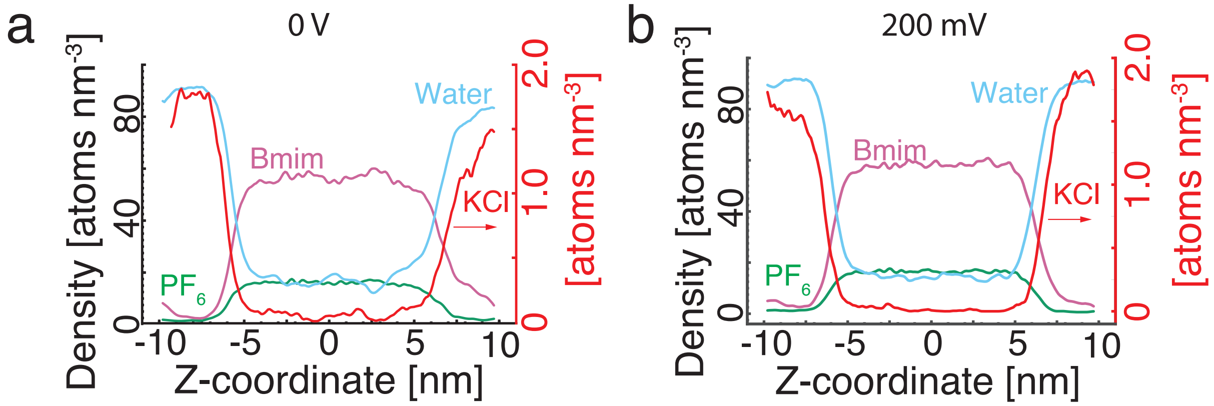

Figure S5. Number density profiles of the molecular species across the two-phase system at the end of a free-equilibration simulation (a) and a simulation carried out under a 200 mV bias (b) applied normal to the IL/AS interface. The profiles were computed from the last 10 ns of the respective simulation trajectories in 1.0 Å bins.

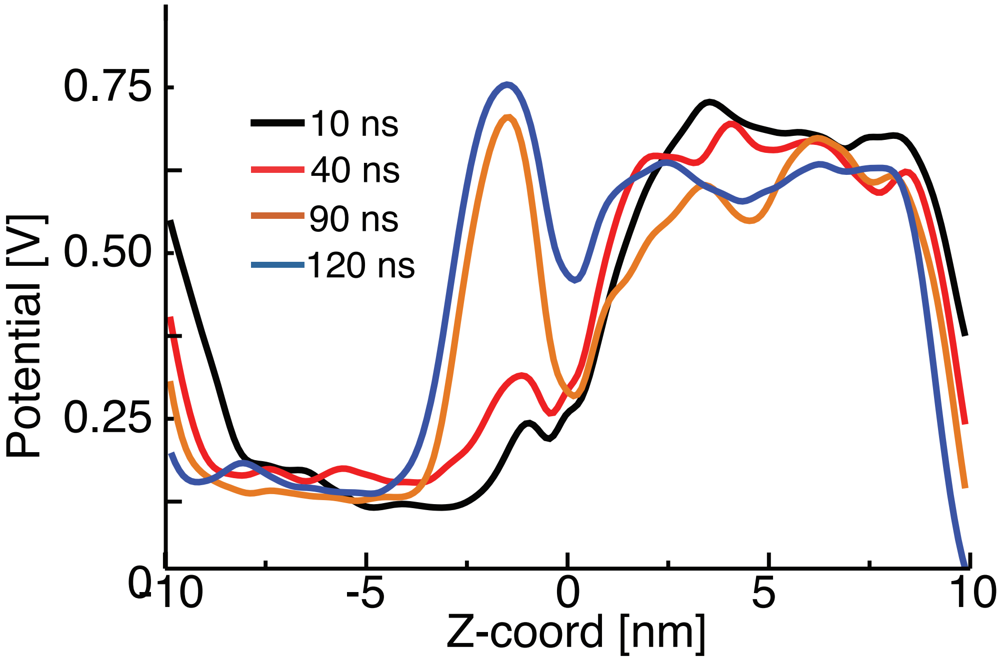

Figure S6. Evolution of the electrostatic potential profile along the symmetry axis of a MoS_2 nanopore across the $[Bmim][PF_6]$/1M KCl interface under a 200 mV transmembrane potential. The final configuration of the simulation system is shown in Figure 3c. The electrostatic potential profiles at 10, 40, 90 and 120 ns were averaged over the preceding 5 ns.

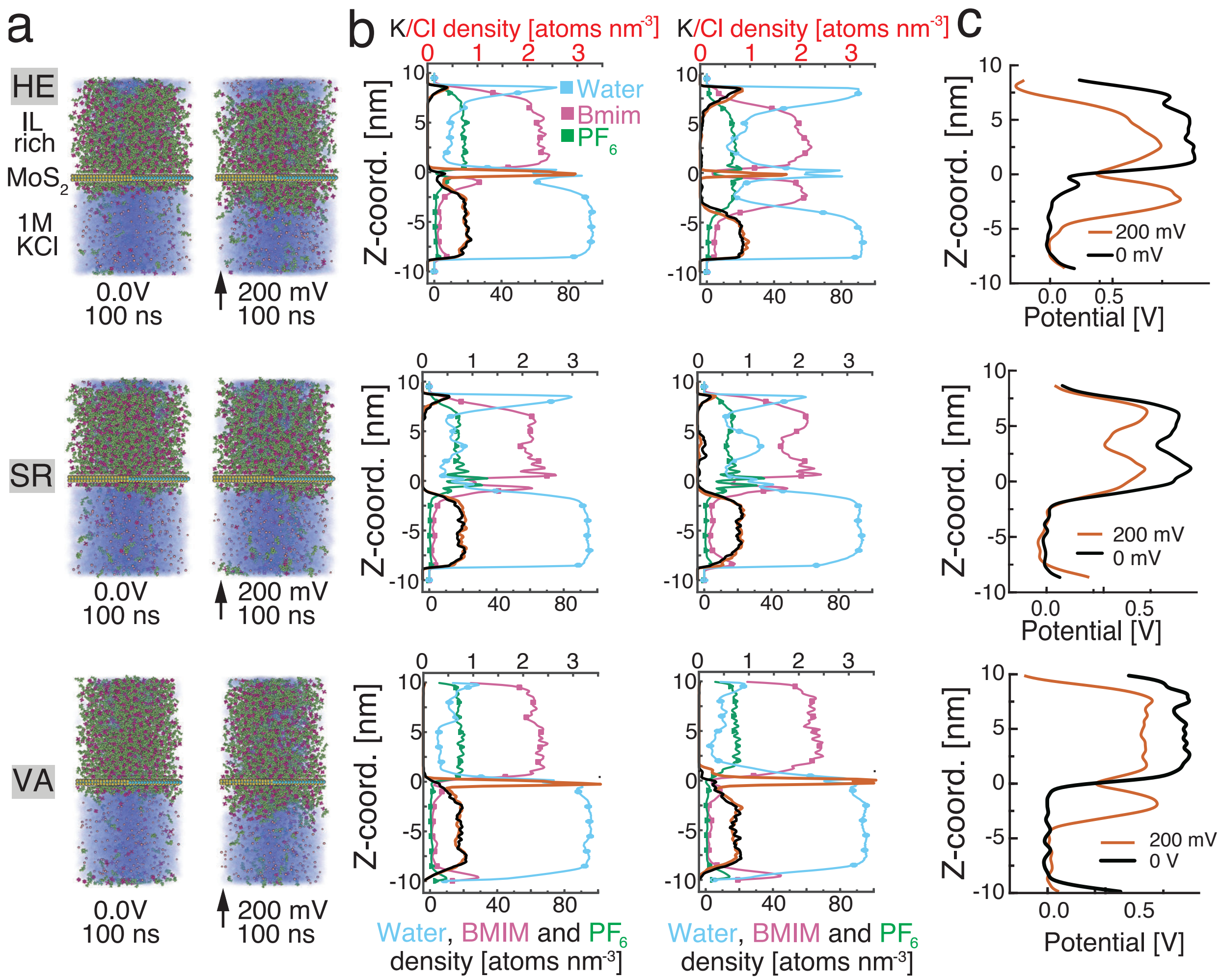

Figure S7. Effect of MoS_2 force field on the distribution of molecular species and the electric potential. The force fields tested are labeled as HE (Heiranian et al) [4], SR (Sresht et al.) [5] and VA (Varshney et al.) [6]. (a) Illustration of the simulation system where an IL-rich region and 1 M KCl are separated by a MoS_2 membrane containing a 2.3 nm nanopore. The left and right snapshots shows the state of the system at the end of a 100 ns equilibration and at the end of a 100 ns applied bias (200 mV) simulation. K and Cl ions are shown as pink vdW spheres, atoms in BMIM and PF_6 as magenta and green spheres, and water is shown as a blue semi-transparent surface. Mo and S atoms of the MoS_2 membrane are shows as cyan and yellow vdW spheres, respectively. (b) Density profiles of the molecular species averaged over the last 5 ns of the 100 ns equilibration (left plot) and over the last 5 ns of the 100 ns applied bias (200 mV) simulation (right plot). The density profiles were obtained by averaging the number density of each component over 1.0 Å bins across the z-axis. Note the scale for the KCl profile is displayed at the top axis. (c) Average electrostatic profiles averaged over the last 5 ns of the 100 ns equilibration (black) and the 200 mV applied bias (red) simulations.

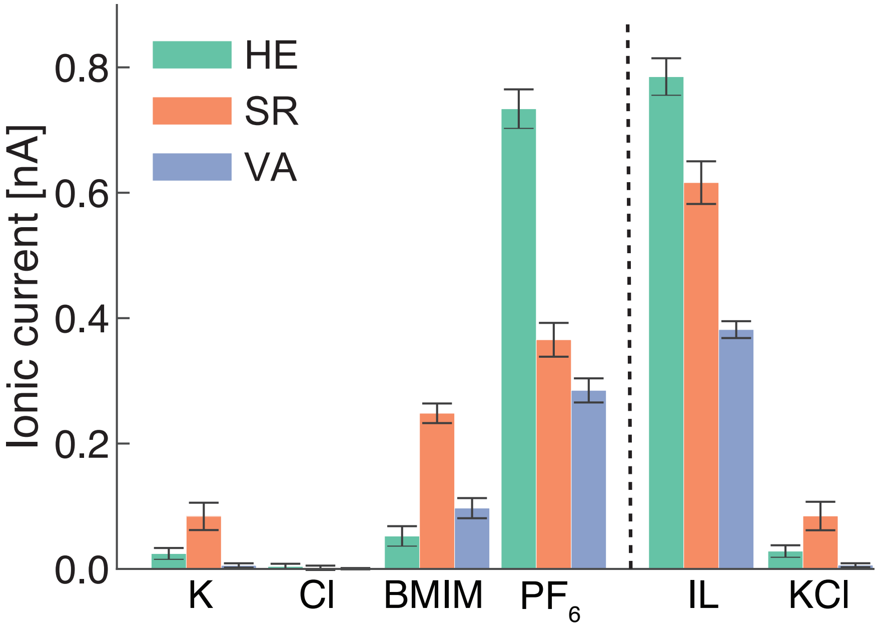

Figure S8. Effect of MoS_2 force field on ionic current magnitude. Ionic currents were measured from 100 ns simulations under a 200 mV bias; the simulation systems are shown in Figure S7. The force fields tested are labeled labeled as HE (Heiranian et al) [4], SR (Sresht et al.) [5] and VA (Varshney et al.) [6].

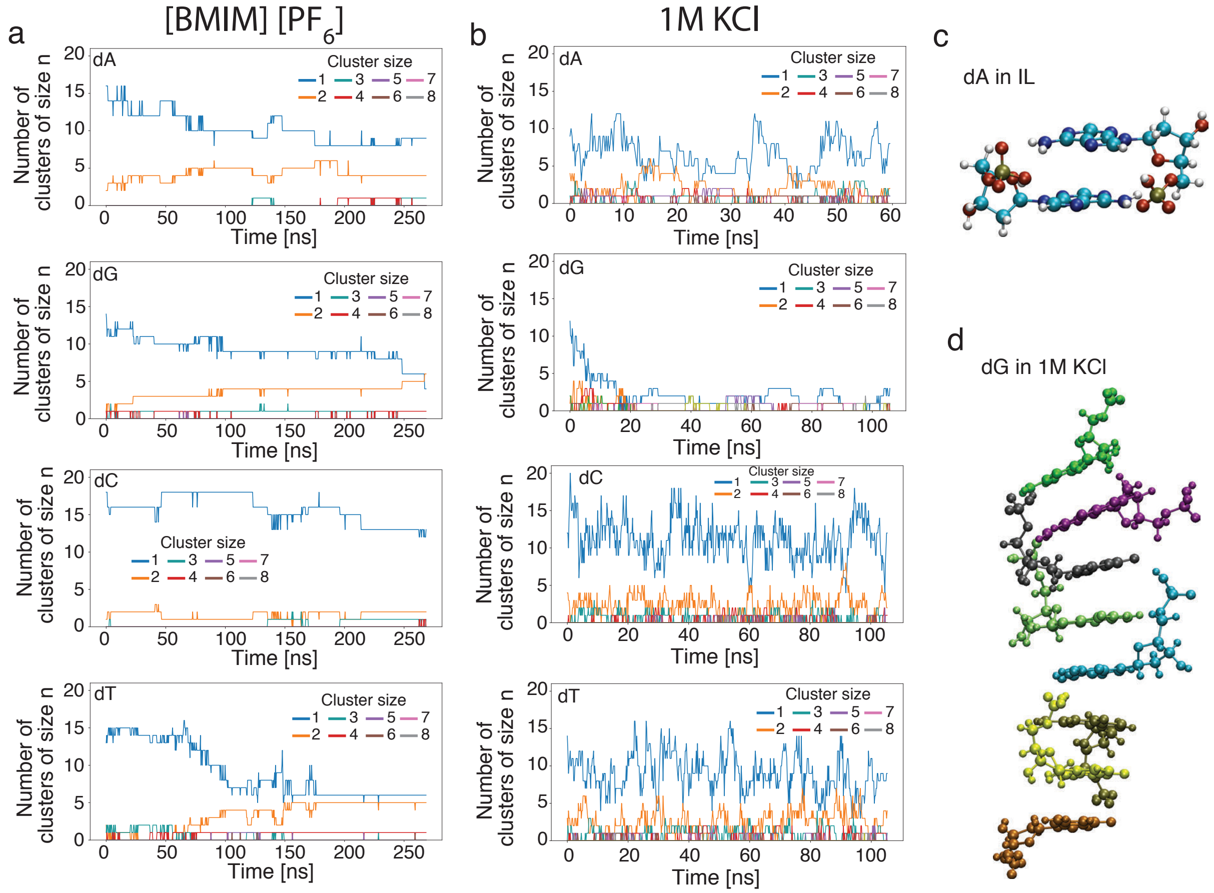

Figure S9. Aggregation propensity of single nucleotides in [Bmim][PF$_6$] and 1M KCl solutions. (a,b) The number of nucleotide clusters containing the specified number of nucleotides in the simulations performed in pure [Bmim][PF$_6$] (a) and 1M KCl (b). Nucleotides within 3.5 Å of each other were counted as forming a cluster. (c) Representative stacking of adenine nucleotides in [Bmim][PF$_6$]. (d) A large aggregate formed spontaneously by dG nucleotides in 1M KCl.

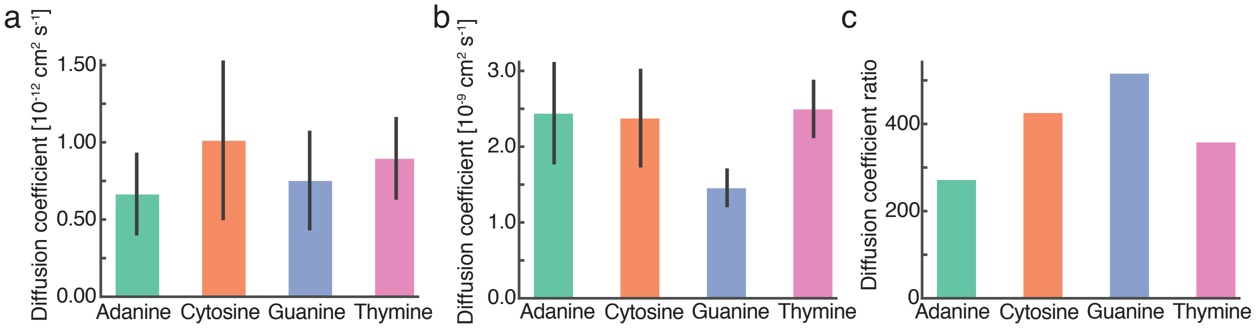

Figure S10. (a) Diffusion coefficients of single DNA nucleotides in pure [Bmim][PF$_6$] obtained from MD simulations. In each simulation, four DNA nucleotides were randomly placed in an box of pure [Bmim][PF$_6$] and simulated for 200 ns. Mean squared displacements (MSD) were calculated from 10 ns segments of the trajectory. The diffusion coefficients were calculated by performing a linear least squares fit to each MSD and taking 1/6 of the slope of the fitted lines. The diffusion coefficients from each of the segments were used to calculate the mean diffusion coefficient. The error bars are the standard deviation of the mean diffusion coefficient. (b) Diffusion coefficient of a single DNA nucleotide in 1M KCl from MD simulations. A single DNA nucleotide was placed in 1M KCl solution and simulated for 200 ns. Mean squared displacements were calculated from 2 ns blocks of the trajectory. (c) Ratio of the diffusion coefficients in pure [Bmim][PF$_6$] and 1M KCl.

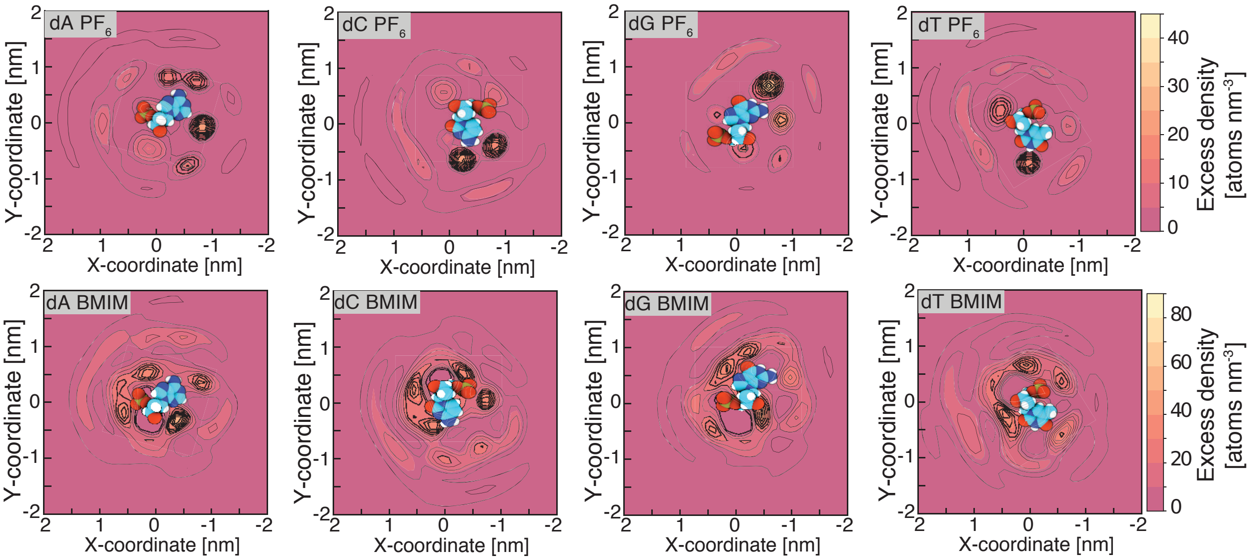

Figure S11. Distribution of BMIM and PF_6 around individual DNA nucleotides. The heat maps illustrate the average mass density of PF_6 and BMIM around adenine, cytosine, guanine and thymine nucleotides. The density maps were obtained from 200 ns MD trajectories of twenty single nucleotides in pure [Bmim][PF_6] by aligning each of the 20 nucleotides to the same reference point and calculating a 1 Å resolution 3D grid of the number density of PF_6 or BMIM around the nucleotide. The average of the twenty density maps was taken to produce one 3D density map. That 3D map was then averaged in the direction normal to the plane of the nucleotides to create a 2D density map within the plane defined by the C2, C4, and C6 atoms of the nucleic acid ring. The average value of the density map was subtracted from the map to emphasize density variation near the nucleotides.

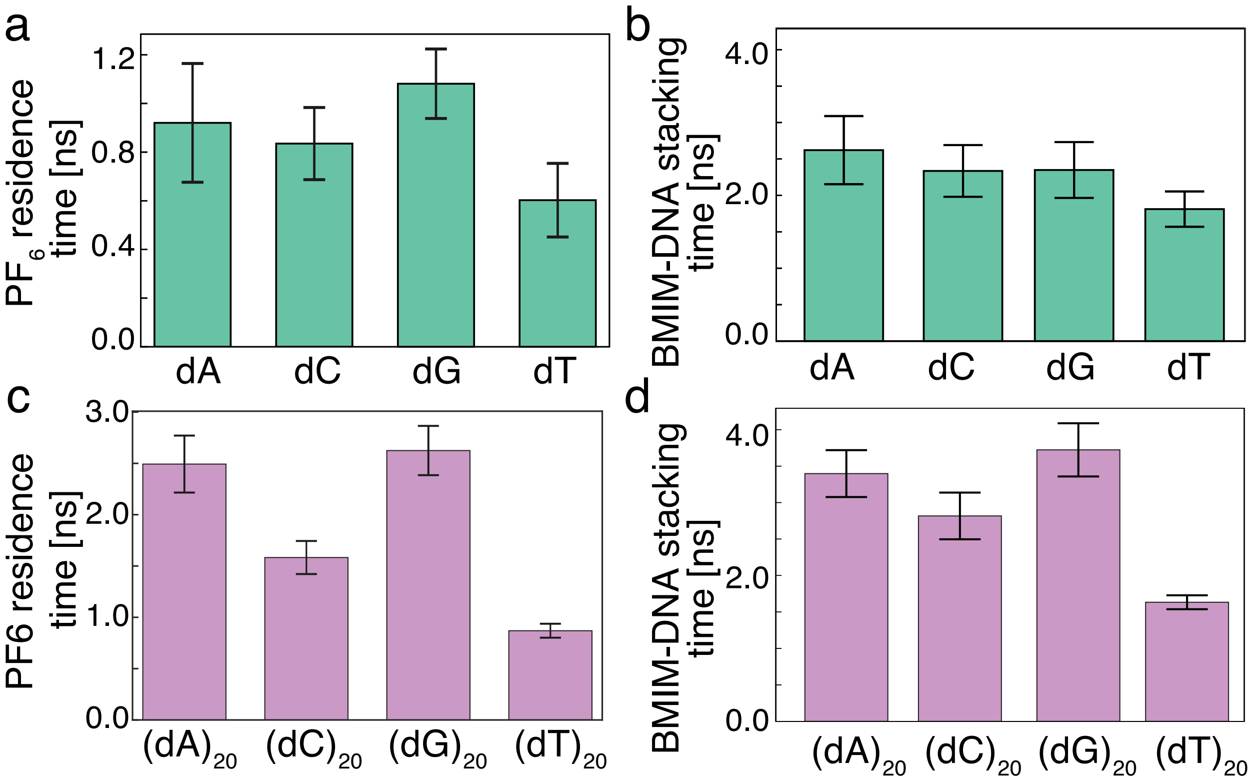

Figure S12. Lifetime of interactions of BMIM and PF_6 with DNA nucleotides. Panels a and c show the average residence time of PF_6 near single nucleotides (a) and individual nucleotides within a DNA homopolymer (c). Panels b and d show the average stacking time of BMIM with single nucleotides (b) and within a DNA homopolymer (d). To calculate the average residence time, the duration of each unique contact between PF_6 or BMIM and a nucleotides was recorded. For PF_6, a 3.6 Å cutoff was used. To count as a stacking interaction, the 3-methylimidazolium head of BMIM molecule must stack on the nitrogenous base of a nucleotide and resided within 5 Å of the DNA base. A BMIM molecule was considered stacked if the vector drawn normal to a plane formed by nucleotide ring atoms N1, N4, N3 and C5 for adenine and guanine bases and N1, C4, C2 and C6 atoms for cytosine and thymine bases was within 11° of the vector drawn normal to a plane formed by the C2, C5 and N3 atoms of the 3-methylimidazolium headgroup of BMIM. Residence and stacking times were calculated separately for each 5 ns fragments of the trajectorites. Distributions of the individual contact durations were fit to exponential functions and the time constants were taken as the residence times. The residence times from each trajectory fragment were used to calculate the average residence time and its standard deviation.

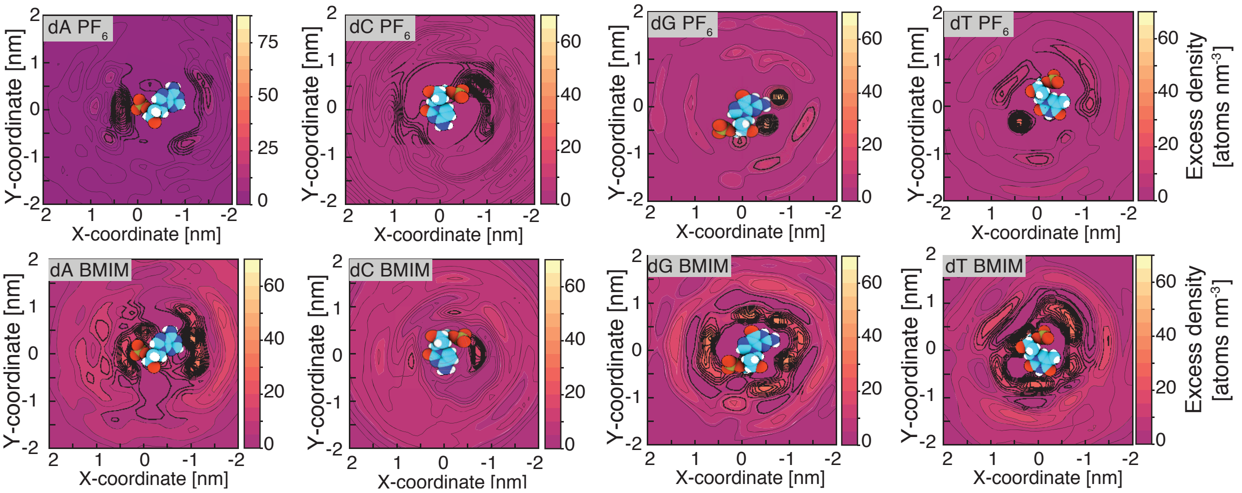

Figure S13. Distribution of PF_6 and BMIM around nucleotides of DNA homopolymers. The density maps were obtained from 200 ns MD trajectories of poly(dA)$_{20}$, poly(dC)$_{20}$, poly(dG)$_{20}$ or poly(dT)$_{20}$ in pure [Bmim][PF_6]. The heat maps were calculated as described in the caption to Figure S11.

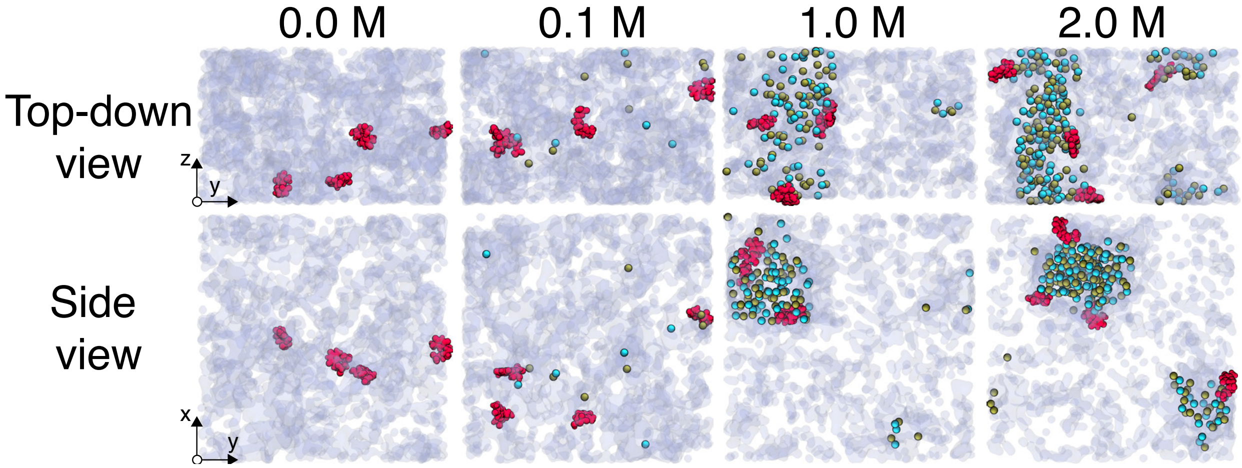

Figure S14. Aggregation of hydrated nucleotides in IL. Final snapshots from MD simulations of four randomly placed thymine nucleotides each hydrated by a 1.5 nm sphere of water molecules. The concentration of KCl was 0, 0.1, 1.0 and 2.0 M in four independent simulations. The snapshots shown were taken at the end of a 150 ns equilibration simulation. Atoms of nucleotides are shown as red vdW spheres whereas potassium and chloride ions are shown in gold and cyan. IL molecules are represented as blue semi-transparent surfaces and water molecules are omitted for clarity.

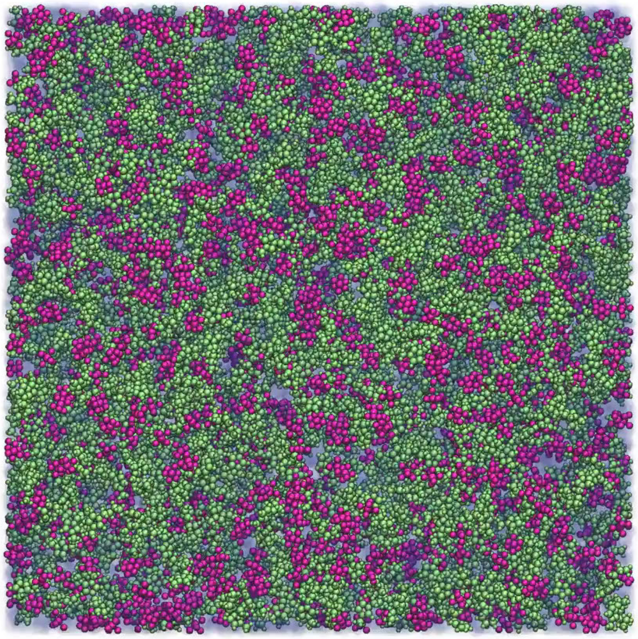

Supplementary Movie 1. Phase separation of initially homogeneously system containing equal volumes of [Bmim][PF_6] and 1M KCl solutions. The movie represents a 160 ns MD trajectory. Spheres illustrate K and Cl ions (pink), atoms of BMIM (green) and PF_6 (magenta); water is shown as a blue semi-transparent surface.

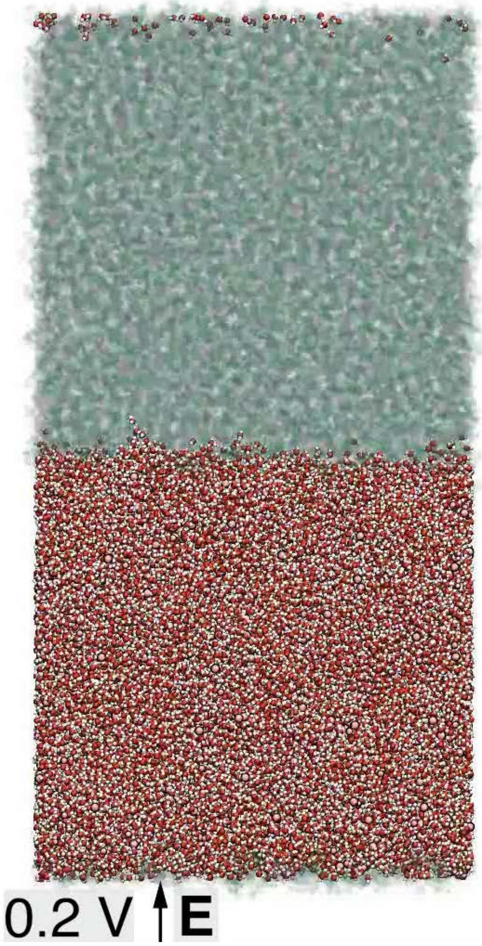

Supplementary Movie 2. Equilibration of a [Bmim][PF_6]/1M KCl system. This equilibrium MD simulation begins with a state where two equal volumes of pure [Bmim][PF_6] and 1M KCl electrolyte are in contact. The movie represents a 170 ns MD trajectory. Red and white spheres illustrate oxygen and hydrogen atoms of water, translucent green and gray spheres correspond to atoms of BMIM and PF_6; pink spheres illustrate K and Cl ions.

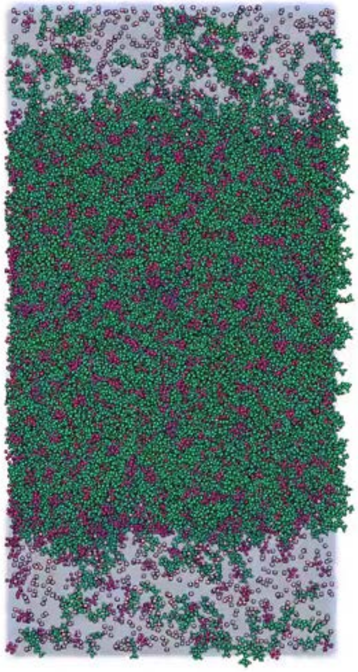

Supplementary Movie 3. MD simulation of the two-phase [Bmim][PF$_6$]/1M KCl system under a 200 mV bias. Atoms of BMIM and PF$_6$ are shown as magenta and green spheres, K and Cl ions in pink, water as a blue semitransparent surface. The simulation begins from a configuration obtained at the end of a 170 ns equilibration (Supplementary Movie 2). The movie illustrates a 120 ns MD trajectory.

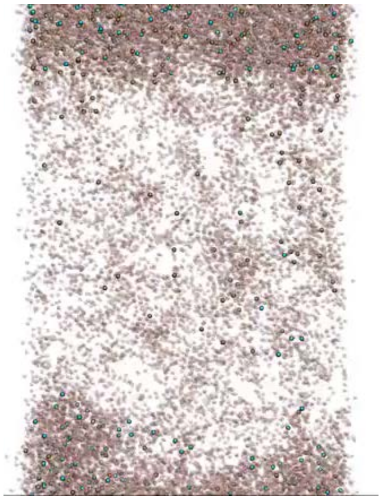

Supplementary Movie 4. Ion transport through water networks in the IL-rich phase. The simulation illustrates the same trajectory as the Supplementary Movie 3, where a 200 mV voltage was applied across the system normal to the IL/AS interface. In this movie, water is represented as red translucent spheres, K and Cl ions as gold and cyan spheres, respectively, whereas BMIM and PF$_6$ are not shown for clarity.

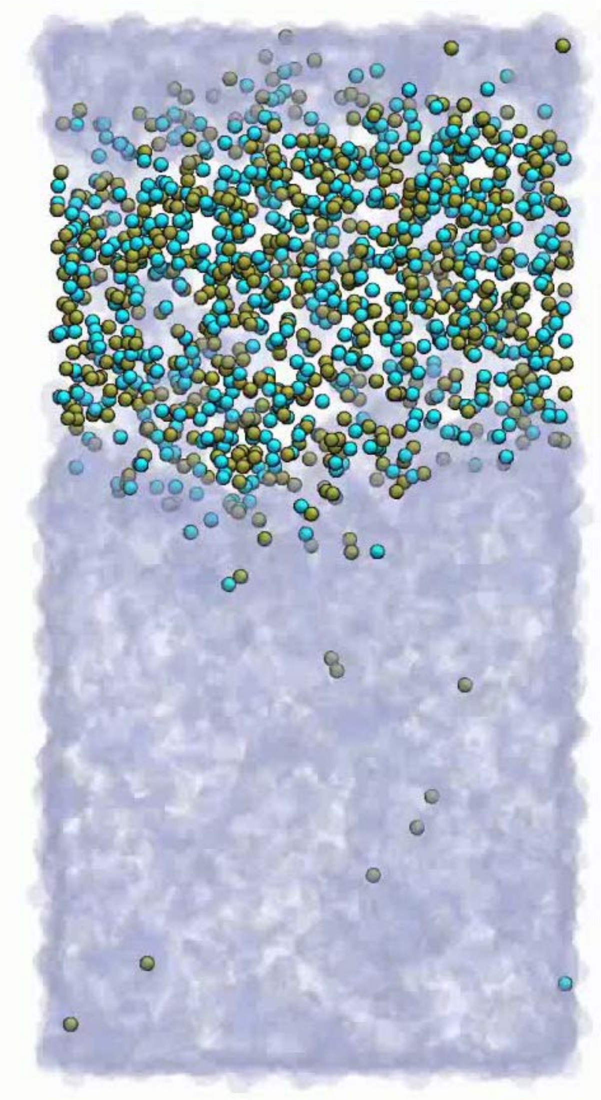

Supplementary Movie 5. Reversible voltage-dependent switching of the interface geometry. Green and blue vdW spheres represent K and Cl ions, respectively, gray represents BMIM and PF_6, water is not shown for clarity. The simulation begins with a two-phase conformation obtained at the end of a 120 ns simulations under a 200 mV bias. A transmembrane bias of 1.0 V is applied for 76 ns. Following that, the system is equilibrated in the absence of external electric field for 100 ns.

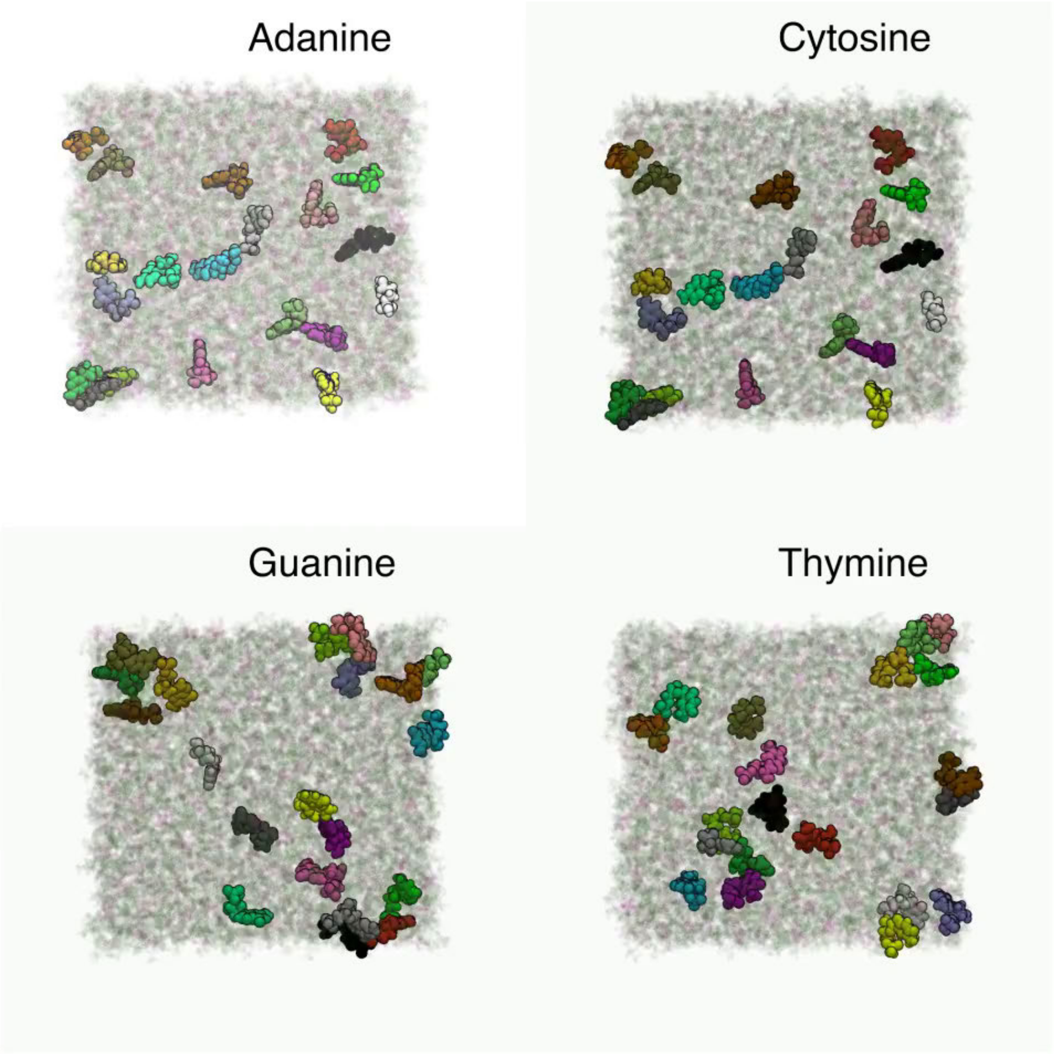

Supplementary Movie 6. Single nucleotide dynamics in [Bmim][PF$_6$]. Twenty adenine, cytosine, guanine and thymine nucleotides were randomly placed in pure [Bmim][PF$_6$] and equilibrated for 260 ns. Each nucleotide is shown in a different color, the atoms of BMIM and PF$_6$ as translucent magenta and green spheres, respectively.

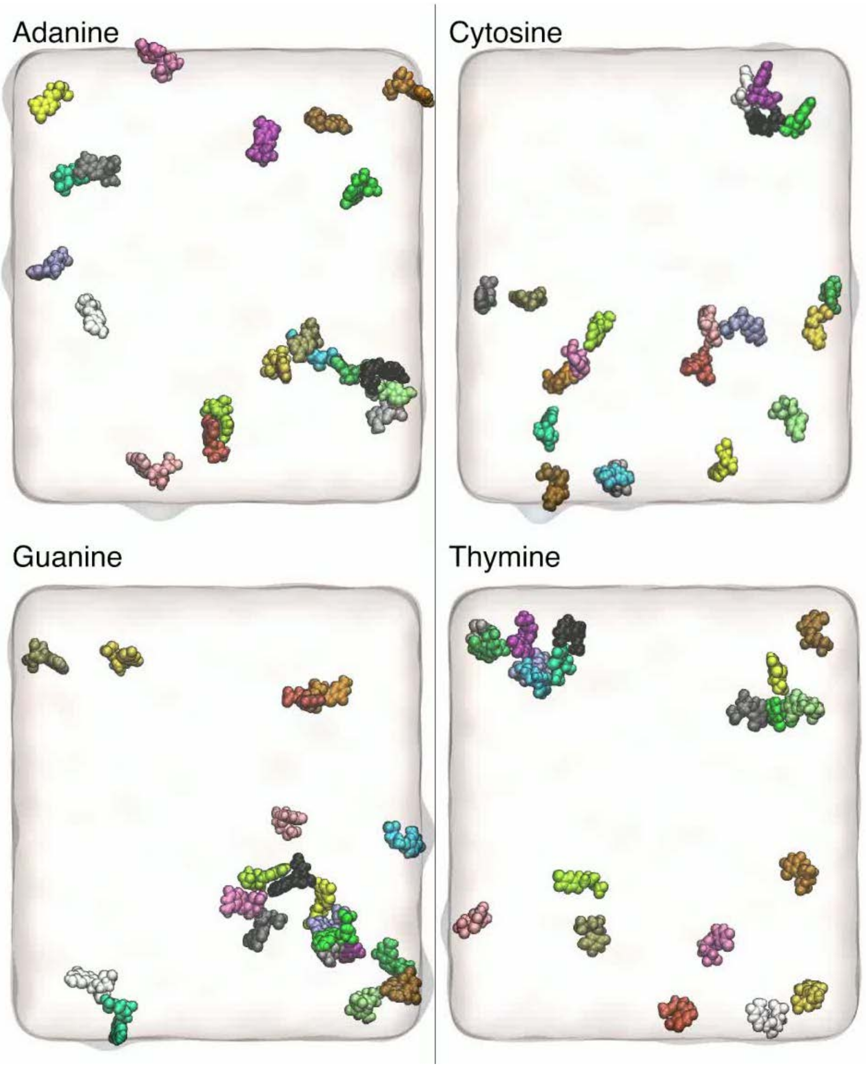

Supplementary Movie 7. Single nucleotide dynamics in KCl solution. Twenty adenine, cytosine, guanine and thymine nucleotides were randomly placed in 1M KCl electrolyte and equilibrated for 100 ns. Each nucleotide is shown in a different color, water as a semitransparent surface. K and Cl ions are not shown for clarity.

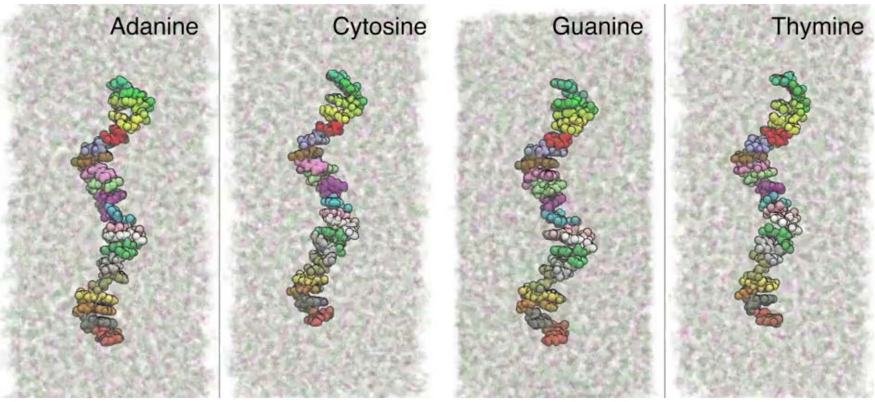

Supplementary Movie 8. Equilibration of DNA homopolymers in pure [Bmim][PF$_6$]. The initial conformation of each homopolymer was taken from a B-form DNA duplex. Each DNA base is uniquely colored and atoms are represented by spheres. BMIM and PF$_6$ molecules are represented by magenta and green translucent spheres, respectively.

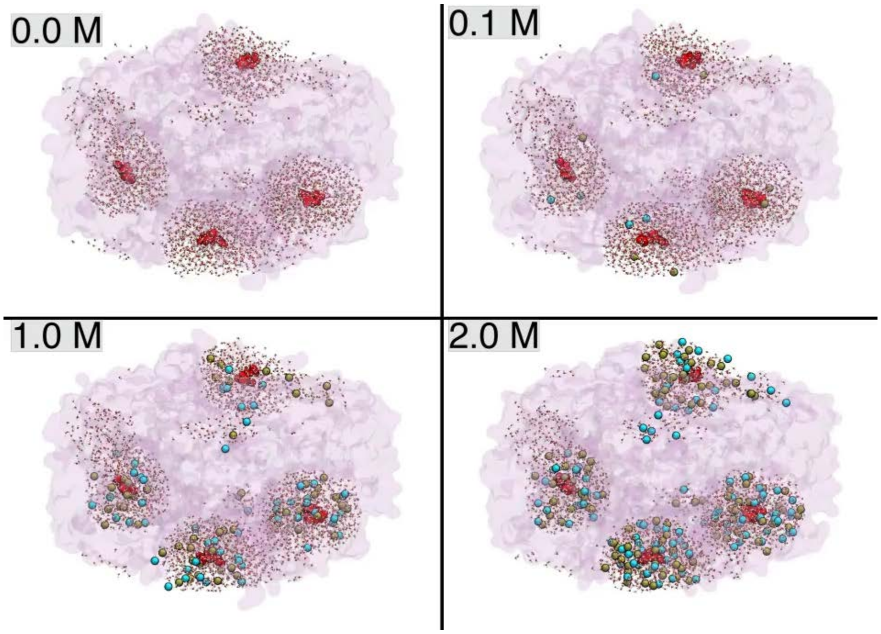

Supplementary Movie 9. Electrolyte-driven aggregation of four hydrated single adenine nucleotides in ionic liquid. Four adenine nucleotides (red spheres) are placed randomly, separated by at least 3 nm. Nucleotides were initially hydrated by a 1.5 nm sphere of water molecules represented as red (oxygen) and white (hydrogen) spheres. The movie illustrates four 150 ns MD trajectories differing by KCl concentration.

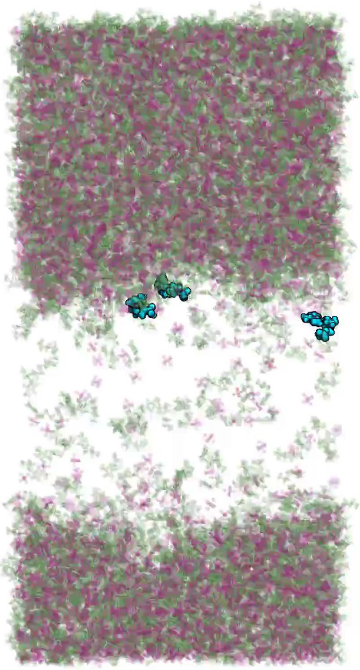

Supplementary Movie 10. MD simulation of three adenine nucleotides in a two-phase system under a 200 mV transmembrane bias. The two-phase system was equilibrated for 100 ns before the nucleotides were insterted at random position. Following that, the system was equilibrated for additional 30 ns. The nucleotides are represented as cyan spheres whereas BMIM and PF_6 are are shown as semitransparent molecules colored in green and magenta. Water and KCl are not shown for clarity. The movie represents a 80 ns MD trajectory.

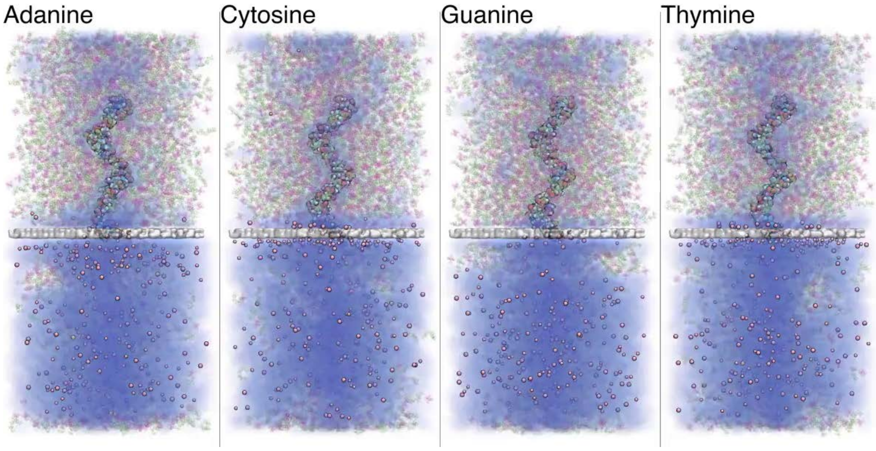

Supplementary Movie 11. Spontaneous transport of ssDNA homopolymers through a MoS_2 nanopore. In each simulation system, a poly(dA)$_{20}$, poly(dC)$_{20}$, poly(dG)$_{20}$ or poly(dT)$_{20}$ strand was inserted into a MoS_2 nanopore system, which was then equilibrated for 15 ns with all non-hydrogen atoms of the DNA constrained to their initial positions. The DNA is shown using spheres colored according to the atom type: blue (nitrogen), red (oxygen), white (hydrogen), carbon (cyan) and gold (phosphorous). This movie represents 190 ns of simulation time.

References

[1] Darve, E. & Pohorille, A. Calculating Free Energies Using Average Force. *J. Chem. Phys.* **115**, 9169–9183 (2001).

[2] Hénin, J., Fiorin, G., Chipot, C. & Klein, M. L. Exploring Multidimensional Free Energy Landscapes Using Time-Dependent Biases on Collective Variables. *J. Chem. Theory Comput.* **6**, 35–47 (2010).

[3] Comer, J. *et al.* The Adaptive Biasing Force Method: Everything You Always Wanted To Know but Were Afraid To Ask. *J. Phys. Chem. B* **119**, 1129–1151 (2015).

[4] Heiranian, M., Wu, Y. & Aluru, N. R. Molybdenum Disulfide and Water Interaction Parameters. *J. Chem. Phys.* **147**, 104706 (2017).

[5] Sresht, V. *et al.* Quantitative Modeling of MoS2–Solvent Interfaces: Predicting Contact Angles and Exfoliation Performance using Molecular Dynamics. *J. Phys. Chem. C* **121**, 9022–9031 (2017).

[6] Varshney, V. *et al.* MD Simulations of Molybdenum Disulphide (MoS2): Force-Field Parameterization and Thermal Transport Behavior. *Comput. Mater. Sci.* **48**, 101–108 (2010).